REPORT DOCUMENTATION PAGE

Form Approved
OMB No. 0704-0188

1. REPORT DATE *(DD-MM-YYYY)*	**2. REPORT TYPE**	**3. DATES COVERED** *(From - To)*
2013	Open Literature	

4. TITLE AND SUBTITLE
Development of a model for nerve agent inhalation in conscious rats

5a. CONTRACT NUMBER

5b. GRANT NUMBER
3.F0014_09_RC_C

5c. PROGRAM ELEMENT NUMBER

6. AUTHOR(S)
Wong, B, Perkins, MW, Santos, MD, Rodriguez, AM, Murphy, G, Sciuto, AM

5d. PROJECT NUMBER

5e. TASK NUMBER

5f. WORK UNIT NUMBER

7. PERFORMING ORGANIZATION NAME(S) AND ADDRESS(ES)

US Army Medical Research Institute of Chemical Defense
ATTN: MCMR-CDT-T
3100 Ricketts Point Road
Aberdeen Proving Ground, MD 21010-5400

8. PERFORMING ORGANIZATION REPORT NUMBER

USAMRICD-P12-037

9. SPONSORING / MONITORING AGENCY NAME(S) AND ADDRESS(ES)
Defense Threat Reduction Agency
8725 John J. Kingman Road STOP 6201
Fort Belvoir, VA 22060-6201

10. SPONSOR/MONITOR'S ACRONYM(S)

11. SPONSOR/MONITOR'S REPORT NUMBER(S)

12. DISTRIBUTION / AVAILABILITY STATEMENT

Approved for public release; distribution unlimited

13. SUPPLEMENTARY NOTES
Published in Toxicology Mechanisms and Methods, 23(7), 537-547, 2013. This work was funded by the Defense Threat Reduction Agency – Joint Science and Technology Office, Medical S&T Division.

14. ABSTRACT
See reprint.

15. SUBJECT TERMS
Chemical warfare, cholinesterases, inhalation exposure, nerve agents, organophosphates, vapor

16. SECURITY CLASSIFICATION OF:			**17. LIMITATION OF ABSTRACT**	**18. NUMBER OF PAGES**	**19a. NAME OF RESPONSIBLE PERSON**
a. REPORT	**b. ABSTRACT**	**c. THIS PAGE**			Alfred M. Sciuto
UNCLASSIFIED	UNCLASSIFIED	UNCLASSIFIED	UNLIMITED	11	**19b. TELEPHONE NUMBER** *(include area code)* 410-436-5115

Standard Form 298 (Rev. 8-98)
Prescribed by ANSI Std. Z39.18

Toxicology Mechanisms and Methods

http://informahealthcare.com/txm
ISSN: 1537-6516 (print), 1537-6524 (electronic)

Toxicol Mech Methods, 2013; 23(7): 537–547
 DOI: 10.3109/15376516.2013.796033

informa healthcare

RESEARCH ARTICLE

Development of a model for nerve agent inhalation in conscious rats

Benjamin Wong, Michael W. Perkins, Mariton D. Santos, Ashley M. Rodriguez, Gleeson Murphy, and Alfred M. Sciuto

Medical/Analytical Toxicology, US Army Medical Research Institute of Chemical Defense, MD, USA

Abstract

This study characterizes the development of a head-out inhalation exposure system for assessing respiratory toxicity of vaporized chemical agents in untreated, non-anesthetized rats. The organophosphate diisopropyl fluorophosphate (DFP) induces classical cholinergic toxicity following inhalation exposure and was utilized to validate the effectiveness of this newly designed inhalation exposure system. A saturator cell apparatus was used to generate DFP vapor at 9750, 10 950, 12 200, 14 625 and 19 500 mg × min/m^3 which was carried by filtered nitrogen into a glass mixing tube, where it combined with ambient air before being introduced to the custom-made glass exposure chamber. Male Sprague-Dawley rats (250–300 g) were restrained in individual head-out plethysmography chambers, which acquired respiratory parameters before, during and after agent exposure. All animals were acclimated to the exposure system prior to exposure to reduce novel environment-induced stress. The LCt_{50}, as determined by probit analysis, was 12 014 mg × min/m^3. Weight loss in exposed animals was dose-dependent and ranged from 8 to 28% of their body weight 24 h after exposure. Increased salivation, lacrimation, urination, defecation (SLUD) and mild muscular fasciculation were observed in all DFP-exposed animals during and immediately following exposure. In all exposed animals, DFP vapor produced significant inhibition of acetylcholinesterase (AChE) activity in cardiac blood, bronchoalveolar lavage fluid (BALF), whole brain and lung tissue as well as alterations in tidal volume and minute volume. These studies have provided valuable information leading to the initiation of studies evaluating inhalational toxicity and treatments following exposure to the more lethal and potent chemical warfare nerve agents.

Keywords

Chemical warfare, cholinesterases, inhalation exposure, nerve agents, organophosphates, vapor

History

Received 21 February 2013
Revised 5 April 2013
Accepted 7 April 2013
Published online 23 May 2013

Introduction

Chemical exposure is an inevitability faced by military and civilian populations alike. History has shown that whether through accidents, natural disasters, acts of terrorism, or warfare, human populations have been threatened by and exposed to chemical warfare agents, toxic industrial chemicals (TICs) and toxic industrial materials (TIMs). These incidents include multiple uses of sulfur mustard in the twentieth century (Abbas, 1984; Feakes, 2003; Maynard & Chilcott, 2009), the 1984 leak of methyl isocyanate gas in Bhopal (Broughton, 2005; Eckerman, 2005) and the 1995 release of sarin on the Tokyo subway (Smithson et al., 2000) and demonstrate the central importance of sufficient preparation and countermeasure strategies in effectively treating and reducing casualties. Although what constitutes sufficient preparation and countermeasure strategies may be partially open to interpretation, that body of knowledge must contain toxicological models capable of accurately describing the onset of toxicity and progression of symptoms. Both of these are widely known to be affected by a multitude of factors, but of particular importance is the nature of the chemical agent, the route of exposure and population characteristics (Anzueto et al., 1986; Benton et al., 2006; Fawcett et al., 2009; Franz & Hilaski, 1990; Kirby, 2005; Mioduszewski et al., 2002b; Niven & Roop, 2004; Rickett et al., 1986).

Acetylcholinesterase (AChE) inhibitors are part of a broad range of compounds consisting of organophosphate pesticides and traditional chemical warfare nerve agents (CWNAs) such as sarin or soman. Exposure to AChE inhibitors results in accumulation of the neurotransmitter acetylcholine (ACh) in central and peripheral nervous tissue, leading to various toxic signs including hypersecretions, respiratory depression, severe seizures, and mortality (Bajgar, 2004; Rickett et al., 1986; Sidell & Borak, 1992). The literature describing existing toxicological models of chemical exposure is predominantly based on subcutaneous, intramuscular, or intravenous exposure. However, historical examples as listed previously, as well as expert opinion (Dunn & Sidell, 1989; Niven & Roop, 2004; Sidell et al., 1997), indicate that inhalation is the most likely route of exposure in a chemical incident. In addition, the at-risk population will be unanesthetized and will consist of individuals of both genders and of all

Address for correspondence: Alfred M. Sciuto, Analytical Toxicology Division, US Army Medical Research Institute of Chemical Defense, 3100 Ricketts Point Road, Aberdeen Proving Ground, MD 21010, USA. Tel: 410 436 5115. Fax: 410 436 1960. E-mail: alfred.mario.sciuto@us.army.mil

Toxicol Mech Methods, 2013; 23(7): 537–547

Abbreviations

AChE, Acetylcholinesterase
ATCH, Acetylthiocholine iodide
BAL, Bronchoalveolar lavage
BTCH, Butyrylthiocholine iodide
CEE, Calculated exposure equivalent
CWNA, Chemical warfare nerve agent
DFP, Diisopropyl fluorophosphates
DTP, 4,4′-dithidiopyridine
ET, Expiratory time
GD, Soman
im, Intramuscular
ip, Intraperitoneal
IT, Inspiratory time
LCt_{50}, Lethal concentration for 50% of the population multiplied by exposure time
MV, Minute volume
OP, Organophosphate
PBS, Phosphate buffered saline
sc, Subcutaneous
SLUD, salivation, lacrimation, urination, defecation
SLPM, standard liters per minute
TIC, Toxic industrial chemical
TIM, Toxic industrial material
TV, Tidal volume

ages. In the United States alone, the young, healthy male is estimated to constitute only 11% (Flegal et al., 2010; U.S. Census Bureau, 2010) of the population. Based on these assessments, a realistic and applicable model for chemical exposure should include the inhalation exposure of conscious subjects and be capable of describing the toxicokinetics and toxicodynamics of a vapor and/or aerosol exposure in a representative population.

The most common inhalation toxicology exposure models are whole-body, head-only, nose-only, lung-only and partial lung (Anthony et al., 2004; Dabisch et al., 2008; Mioduszewski et al., 2002a; Muse et al., 2006), each with distinct utility. This study developed a head-out, vapor-generating inhalation exposure system for conscious Sprague-Dawley rats, since the primary advantage of a head-only inhalation exposure model is the ability to perform repeated and brief exposures while limiting pathways of agent entry into the animal (Phalen, 1976). This study also aimed to provide more realistic exposure results by utilizing untreated and non-anesthetized animals. Mortality, clinical observations, body weight loss, AChE inhibition and real-time pulmonary dynamics were used to demonstrate inhalation toxicity of the organophosphate diisopropyl fluorophosphate (DFP), which is structurally similar to CWNAs but is less toxic (Gupta et al., 1985). This work describes a more realistic and relevant CWNA inhalation model that will assist in developing and evaluating therapeutic countermeasure strategies, as well as provide a reliable method by which other chemical threat agents, TICs and TIMs may be examined as inhalational threats.

Materials and methods

Chemicals

Diisopropyl fluorophosphate (DFP, CAS# 55-91-4, ≥97% pure), heparin, acetylthiocholine iodide (ATCH), 4,4′-dithidiopyridine (DTP) were obtained from Sigma-Aldrich (St. Louis, MO). Saline solution and bicinchonic acid (BCA) protein assay kits were purchased from Pierce Chemical Co. (Rockford, IL). Exposure to DFP was performed in an approved fume hood with the appropriate personal protective equipment for the handling of CWNAs. At the end of all vapor exposures and prior to disposal, any remaining DFP and materials contaminated with DFP were decontaminated using a 10% sodium hydroxide solution.

Exposure system configuration

This study utilized a custom-built exposure system consisting of two head-out animal restraint units with integrated plethysmography transducers. These were attached to a larger, main exposure chamber (Figures 1–4). The airflow control system consisted of an industrial automation controller (0154, Brooks Instruments, Hatfield, PA) and 0–30 SLPM and 0–15 SLPM flow controllers (SLA5850, Brooks Instruments) to control exhaust flow from the system and nitrogen flow to the saturator cell, respectively. Agent vapor was generated from a saturator cell which was fed from a mass flow controller that regulated flow (0–5 SLPM) from the nitrogen source through the saturator cell. After exiting the saturator cell, the agent vapor entered the main exposure chamber, in which airflow was determined by the exhaust flow, set at 7.5 SLPM. Each of the head-out restraint/plethysmography units attached to the exposure chamber was used to monitor animal pulmonary function (Muse et al.,

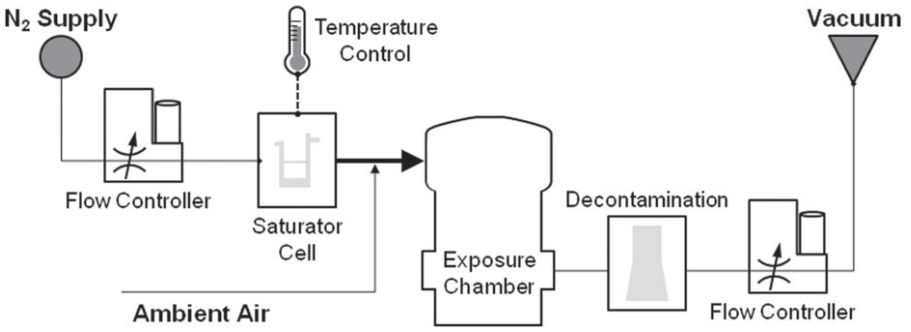

Figure 1. Configuration of head-out vapor exposure system.

Figure 2. DFP vapor-generating saturator cell.

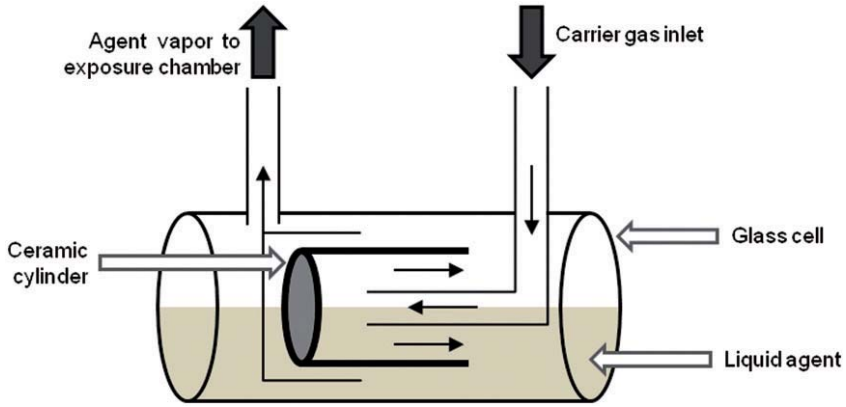

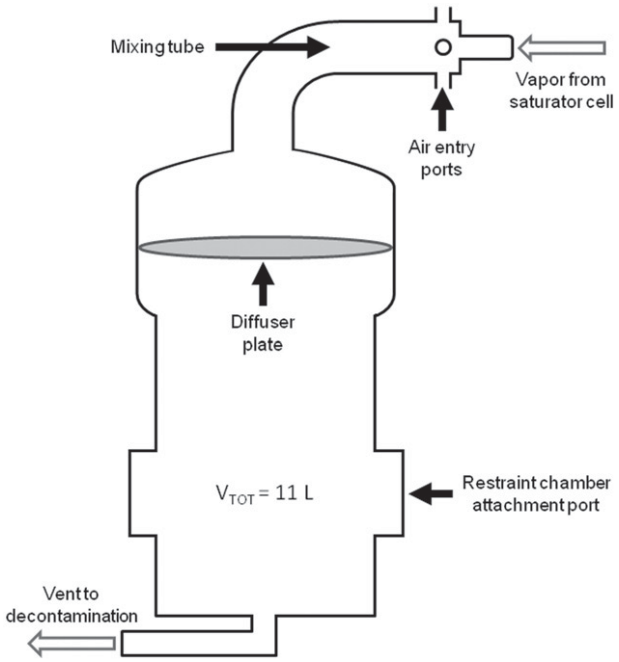

Figure 3. Vapor inhalation exposure chamber. Air flows from top to bottom and is exhausted to decontamination from the bottom. Airflow direction is indicated by the large arrows, and the total volume of the exposure chamber and mixing tube was approximately 11 L.

2006). Agent vapor exiting the exposure chamber was decontaminated in a 2.5% sodium hypochlorite solution and passed through an activated charcoal filter before being vented.

Saturator cell agent generation

The saturated agent vapor streams were generated by flowing nitrogen carrier gas through a glass, multipass vessel containing liquid agent (Figure 2). The saturator cell (Glassblowers.com Inc., Turnersville, NJ) consisted of a 100 mm long, 25 mm OD cylindrical glass tube with two vertical 7 mm OD tubes connected at either end. Contact area between the agent and carrier gas was increased by the placement of a hollow ceramic cylinder (Alundum-fused alumina [Al_2O_3 >90%] Saint-Gobain Ceramics & Plastics Inc., Worchester, MA) within the main body of the saturator cell such that carrier gas was required to make two passes along the surface of the wetted ceramic cylinder before exiting.

The saturator cell was filled with 0.5–1 mL of neat liquid DFP (98% pure) before introduction of the nitrogen carrier gas at a low flow rate (1–2 SLPM). This combination of agent volume and gas flow rate generated saturated vapor for approximately 3–4 exposures of 20 min each.

Vapor inhalation exposure chamber

The exposure chamber (Glassblowers.com Inc., Turnersville, NJ) was a large cylindrical unit constructed of glass (Figure 3). The concentrated agent stream generated in the saturator cell entered at the top of the main exposure chamber through a glass mixing tube (Glassblowers.com Inc.). Four small holes placed at the end nearest the vapor stream allowed entry of ambient air to dilute the concentrated agent vapor. Mixing throughout the exposure chamber was assisted by the placement of a perforated diffuser plate between the vapor entry and restraint chamber attachment ports, which were located near the bottom of the chamber and into which the animal restraint units were inserted. The total volume of the exposure chamber and mixing tube was approximately 11 L.

Head-out animal restraint chambers equipped with plethysmography units

A single plethysmography unit (600-2100-001, Data Sciences International, St. Paul, MN) consisted of two cylindrical clear plastic halves with a cross-sectional diameter of 10 cm and total length of 32 cm (Figure 4). The front half restrained the rodent in a head-out fashion using polyurethane neck seals and a removable, adjustable polymer push rod squeeze-plate mechanism. The rear half was fitted with a pressure transducer (DP45 ± 2.25 cm H_2O, Validyne, Northridge, CA) used to measure various parameters of pulmonary function, as described below. Each Validyne pressure transducer (one per chamber) was secured to a ring stand and clamp. The two halves were held together by clamping locks, and the combined unit was joined to the exposure chamber.

Age-matched, conscious, restrained Sprague-Dawley rats were placed into the chambers such that their heads protruded through a hole in the pre-cut polyurethane neck collar (D = 2 cm), fitted to ensure an airtight seal and simultaneously preventing escape from the chamber through the neck collar. Rats were secured within the chamber using the push rod squeeze-plate mechanism, with their tails threaded through one of the openings in the plate. The two halves of

Toxicol Mech Methods, 2013; 23(7): 537–547

Figure 4. Head-out animal restraint chamber with plethysmography unit.

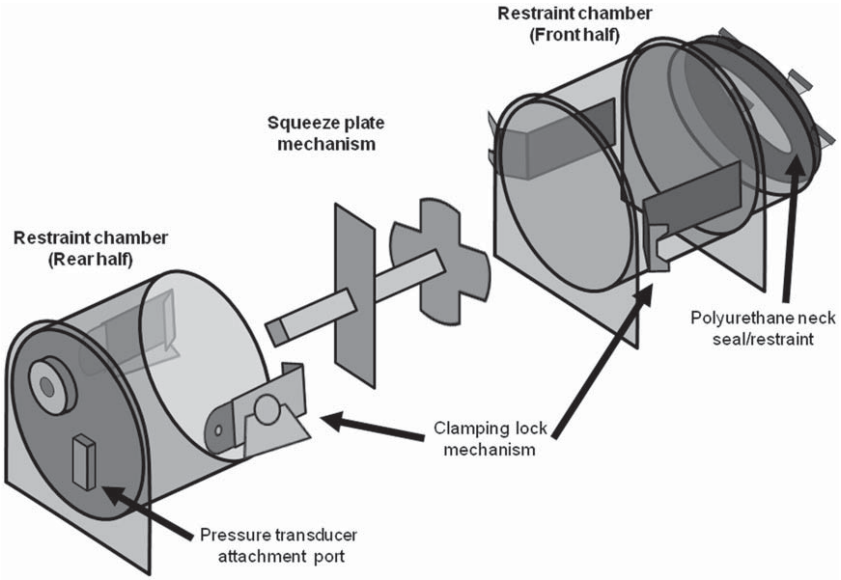

the chamber were then sealed together using the latching mechanisms on the rear half of the head-out chamber assembly.

Changes in chamber pressure, caused by chest movement experienced during breathing while inside the plethysmography chamber, were detected by the pressure transducer and used to monitor various parameters of respiratory function. The respiratory dynamics parameters that were measured were peak inspiratory flow (PIF) and peak expiratory flow (PEF; the maximum inspiratory and maximum expiratory flow rates occurring in one breath), inspiratory (IT) and expiratory (ET) time (the time spent inhaling and exhaling during each breath), tidal volume (TV; the volume of air inspired in a single breath) and minute volume (MV; the product of tidal volume and respiratory rate calculated on a breath-by-breath basis). All respiratory data were collected by the 7700 Platform and Ponemah Performance Analysis software (data acquisition hardware: ACQ7700XE, software: Ponemah v.4.9, Data Sciences International, Valley View, OH). Immediately before exposure, all rats' respiratory parameters were allowed to stabilize during a pre-exposure chamber acclimation period of 10 min. Respiratory parameter readings were then recorded for each animal before exposure (10 min), during exposure (20 min), and during off-gassing (10 min). Data were continuously analyzed in real time during baseline, exposure and off-gassing with data collection occurring at 15 s intervals. The system analysis and acquisition software utilized a rejection index to exclude statistical inaccuracies and external noise.

Exposure dose assessment

The determination of exposure dose was performed by correlating agent use with experimental time. For our system, m_{DFP}, the mass of agent consumed during an experiment was:

$$m_{DFP} = F_e \times C_e \times t$$

where F_e is the flow rate of carrier gas exiting the saturator cell, C_e is the concentration of DFP in the saturated exit stream, and t is the total time during the experiment when carrier gas is passed through the cell. In this experiment, F_e was the only controlled variable, with experimental time set at $t = 20$ min and C_e, determined by the temperature of the saturator cell, set at $T = 22.5\,^{\circ}C$. Further details can be found in Appendix B. At each of the five F_es corresponding to the five doses selected for this experiment, the calculated mass of agent to be used was placed in the saturator cell. Across multiple exposures using different flow rates, all agents added to the saturator cell were vaporized within the allotted time. This result was confirmed by adding excess agent and determining the mass difference in the saturator cell before and after exposure.

Calculated exposure equivalent

We define the calculated exposure equivalent (CEE) as a ratio of the mass of delivered agent to the body mass at exposure. The CEE represents the time-dependent amount of agent delivered to an animal over the course of an inhalation exposure expressed in mg of agent per kg of body weight (mg/kg), the same units used to describe an instantaneous exposure administered through intravenous (iv), intraperitoneal (ip), or subcutaneous (sc) routes. The CEE is also analogous to a delivered dose in inhalation drug administration and is similarly derived and calculated (Alexander et al., 2008).

In brief, the amount of agent delivered to an animal (m_{Ag}, mg) can be calculated from the respiratory minute volume (MV, mL/min), concentration of agent inside the exposure chamber (C_{EXP}, mg/m^3), the time of exposure (t_{EXP}, min) and the inhaled fraction of agent (IF_A). Unlike an aerosol exposure in which deposition in the lungs is based on particle size, the dispersed nature of the agent in a vapor exposure allows for the assumption that the agent is sufficiently well-distributed such that the inhaled fraction is 100% ($IF_A = 1$) at all times. Normalizing for body weight (m, kg) yields the time-dependent expression of CEE as determined by dimensional analysis:

$$CEE = \int_0^{t_{EXP}} \frac{MV(t) \times C_{EXP}(t) \times IF_A(t)}{m(t)} \mathrm{d}t$$

A simplified expression for the CEE can be determined if MV and C_{EXP} are sufficiently weak functions of time and is expressed as follows:

$$\overline{CEE} = \frac{\overline{MV} \times \overline{C_{EXP}} \times t_{EXP}}{\bar{m}}$$

Animal experimentation

A total of 36 (6 naïve control rats and 6 rats for each of the 5 DFP doses) male Sprague-Dawley rats (250–350 g, Charles River Laboratories, Wilmington, MA) were used for this study. Animals were housed individually under standard conditions with a 12 h light/dark cycle and food and water available *ad libitum*. Rats were quarantined for 1 week upon arrival on-site and acclimated to the restraint chamber and exposure system for a total of 7 days for 5–30 min each day to reduce novel environment-induced stress. Animals that failed to successfully acclimate to the exposure system after the 7-day training session were removed from the study.

For exposures, each animal was placed in a restraint chamber, and the chamber inserted into the main exposure unit. Following a 10-min adjustment period and collection of baseline pulmonary dynamics, exposure to DFP vapor was initiated. Animals remained conscious throughout the 20-min exposure and remained within the inserted restraint chamber following the end of the vapor exposure for an additional 10-min off-gassing period. Respiratory parameters were recorded during each of these time intervals. At the conclusion of the off-gassing period, surviving animals were returned to their cages and observed for 24 h. At 24 h post-exposure, animals were returned to the restraint chambers for 10 min to record respiratory parameters and then anesthetized using an im injection of ketamine (90 mg/kg) in combination with xylazine (10 mg/kg). The thoracic cavity was opened and exsanguination performed via cardiac puncture. Tissues (blood, whole brain, and lung) and bronchoalveolar lavage fluid (BALF) were collected for analysis.

All research was conducted in compliance with the Animal Welfare Act and other federal statutes and regulations relating to animals and experiments involving animals. It adhered to principles stated in the *Guide for the Care and Use of Laboratory Animals*, National Research Council, published by the National Academy Press, 1996, and the Animal Welfare Act of 1966, as amended. The study protocol was approved by the Institutional Animal Care and Use Committee, United States Army Medical Research Institute of Chemical Defense (USAMRICD), Aberdeen Proving Ground, MD.

Clinical/observational signs and body weight loss

All animals were monitored for clinical signs during (15 min) and directly after (within the first hour) DFP inhalation exposure. Clinical signs including salivation, lacrimation, urination, defecation (SLUD) percentage weight loss, facial clonus, and convulsions were monitored and recorded for each animal. All surviving animals were evaluated post-exposure for their appearance, general movement, natural behavior and provoked response. Animals were weighed immediately prior to agent exposure and then again before euthanasia (at the 24 h endpoint, before administration of anesthesia) to calculate the percentage body weight loss.

Bronchoalveolar lavage (BAL)

Animals surviving to 24 h after vapor exposure were anesthetized intramuscularly with ketamine (90 mg/kg) and xylazine (10 mg/kg). The thoracic cavity was opened and exsanguination performed by cardiac puncture. BAL was obtained by lavaging the lungs 3 times with 3 ml of oxygen-free saline. BAL cells (BALC) were separated from BAL fluid (BALF) by centrifugation at 2000 rpm for 10 min using a Sorvall table top centrifuge. The average volume of BAL recovered was 2.0 ml.

Blood and BALF AChE activity assay

AChE activity of the blood and BALF were determined using the Walter Reed Army Institute of Research (WRAIR) cholinesterase assay (Ellman et al., 1961; Haigh et al., 2008). Sample aliquots of 10 µL, diluted 9-fold in distilled water for blood samples, were placed in a 96-well microtiter plate. An additional 290 µL of working solution consisting of 50 mM sodium phosphate buffer (pH 8.0), 1 mM acetylthiocholine iodide (ATC) and 0.2 mM of the chromophore 4,4′-dithidiopyridine (DTP) were added to yield a final volume of 300 µL in each well. All samples were thoroughly mixed for 60 seconds, and 10-min kinetic assays (30-second intervals including 3 seconds of shaking) were performed at 324 nm. All spectrophotometric readings were taken on a microtiter plate reader at 25 °C using Spectra Max and Softmax Plus 4.3 LS software (Molecular Devices, Sunnyvale, CA). Blood AChE activity was determined by the average activities (run in triplicate) of all of the fractions. BALF AChE activity was normalized to the protein concentration (as described below in *Protein analysis*), and all AChE activity was expressed as a percentage of the untreated control.

Lung/whole brain collection and AChE activity assay

Animals surviving 24 h after exposure were anesthetized and euthanized as previously described. Following collection of BALF, the left lung lobe was removed, immediately frozen in liquid nitrogen and stored at −80 °C. Animals were then decapitated, and brains were collected, frozen in liquid nitrogen and stored at −80 °C. The left lung lobes and whole brains were homogenized at a 1:7 ratio of tissue protein extraction reagent: buffer volume while on ice using 6–10 short bursts from an Omni Prep multi-sample homogenizer. Homogenates were centrifuged at 4 °C for 10 min at 14 800 rpm using a Fisher Scientific accuSpin micro 17R microcentrifuge. The supernatant was decanted and immediately stored at −80 °C. until subsequent analysis. AChE activity was normalized to the protein concentration and determined as described above.

Protein analysis

Protein levels in the BALF, lung and whole brain homogenates were determined by a BCA protein assay (Pierce Chemical Company, Rockford, IL). Twenty microliters of BALF, lung and whole brain tissue homogenates were directly used to determine protein concentrations using a Spectramax Plus microplate reader and Softmax Plus 4.3 LS software.

Table 1. Clinical/behavioral comparison of control- and DFP vapor-exposed animals.

	DFP exposure dose [mg × min/m^3]					
Parameter	Control	9750	10 950	12 200	14 625	19 500
Survival	6/6	6/6	3/6	3/6	1/6	0/6
Weight loss (%)[a]	-0.5 ± 0.4	8.2 ± 1.3[b]	11.0 ± 0.7[b]	10.1 ± 1.2[b]	$28.1 \pm$ N/A	N/A
Salivation	None	Minor changes	Significant increases	Prominent	Prominent	Prominent
Lacrimation	None	Minor changes	Significant increases	Significant increases	Significant increases	Prominent
Defecation/Urination	Normal	Normal	Significant increases	Significant increases	Prominent	Prominent
Convulsions	None	Minor changes	Significant increases	Significant increases	Prominent	Prominent
Facial clonus	None	Minor changes	Minor changes	Significant increases	Prominent	Prominent
Protrusion of the eye	None	No	Yes	Yes	Yes	Yes
Rearing of hind legs	None	No	No	Yes	Yes	Yes
Appearance[a]	Normal	Normal	Lack of grooming	Lack of grooming	Lack of grooming	None
Movement[a]	Normal	Normal	Incomplete hind limb paralysis	Incomplete hind limb paralysis	Incomplete hind limb paralysis	None
Natural behavior[a]	Normal	Minor changes	Less alert	Less alert	Less alert	None
Provoked response[a]	Normal	Moderate changes	Very weak	Very weak	Very weak	None

[a]Observations taken 24 h post-exposure; [b]$p < 0.05$.

Data analysis

Statistical analyses of differences were performed using the GraphPad Prism V5.04 software (Graph Pad Software Inc., San Diego, CA). For each parameter at each of the three time points (pre-exposure, exposure, and 24 h post-exposure), 1-way ANOVA tests followed by Tukey's test were used to calculate the p values, and probability (p) values less than or equal to 0.05 were considered significant.

Results

Toxic response to agent exposure

Vapor-induced lethality and clinical observations following inhalation exposure to DFP are summarized in Table 1. Animals were exposed to varying concentrations of DFP for 20 min. Data were successfully collected from the head-out plethysmography chambers before, during and after exposure to DFP. All subjects exposed to 19 500 mg × min/m^3 of DFP died, while all exposed to 9750 mg × min/m^3 survived. Survival rates at 24 h after exposure to 10 950, 12 200, and 14 625 mg × min/m^3 were 50%, 50%, and 17%, respectively. The LCt50 as determined by probit analysis was 12 014 mg × min/m^3 (Figure 5). All control animals showed no overt signs of toxicity.

All animals exposed to DFP lost a percentage of their body weight 24 h after inhalation exposure, with surviving animals averaging 9.4% body weight loss, with a single survivor exposed to a high dose (14 625 mg × min/m^3) suffering a 28% loss. Clinical observations recorded during and directly after (1 h) DFP exposure showed a dose-dependent increase in the clinical observations evaluated in this study. None of the recorded clinical or behavior observations were seen in any of the control animals. Initial signs of intoxication were chewing, licking and increased urination and defecation, followed by lacrimation. Intoxication immediately advanced into facial clonus and copious secretions in the oral, then nasal cavities, which then progressed rapidly into gasping for air and convulsions. Rats began to exhibit signs of cholinergic intoxication 3–9 min after the start of DFP exposure.

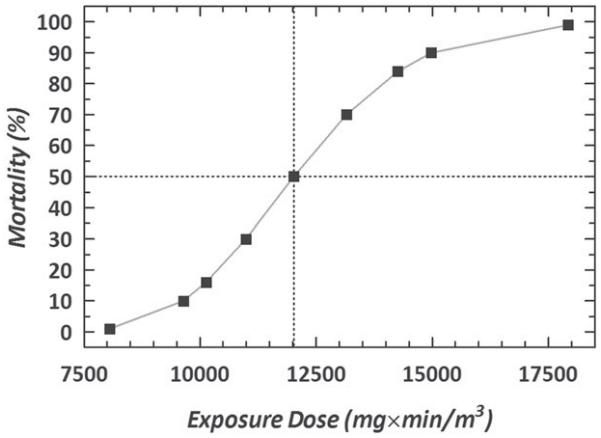

Figure 5. Lethality of DFP vapor in rats. Determined by probit analysis at 24 h post-exposure, with $N = 6$ for each dose (Control/Air, 9750, 10 950, 12 200, 14 625, and 19 500 mg × min/m^3 DFP).

Animals exposed to 14 625 and 19 500 mg × min/m^3 of DFP, all of which exhibited prominent convulsions, died within 17–25 min. All DFP-exposed animals experienced muscular fasciculation to varying degrees, with animals exposed to 12 200, 14 625, and 19 500 mg × min/m^3 experiencing them throughout their entire body. All animals that did not survive the duration of exposure produced copious salivation, exhibited convulsions and experienced severe respiratory distress, as observed and recorded via plethysmography.

Inhibition of AChE activity in various tissues following inhalation exposure to DFP

The inhibition of AChE activity in the blood, BALF, whole brain and lung tissues 24 h post-exposure to DFP is shown in Figure 6. At 24 h after exposure, all surviving animals exposed to 9750, 10 950, and 12 200 mg × min/m^3 of DFP exhibited significant ($p < 0.05$ for each when compared to control) decreases in blood AChE activity. The single animal that survived exposure to 14 625 mg × min/m^3 of DFP exhibited an 84.2% inhibition in blood AChE activity as

compared to the control (unexposed) animal group. Similar inhibition trends were observed in the BALF, brain and lung at all doses.

Respiratory dynamics following inhalation exposure to DFP

Respiratory parameters (PIF, PEF, IT, ET, TV, and MV) were measured by head-out plethysmography before, during and 24 h after exposure in rats exposed to controls and various concentrations of DFP (Table 2). There was a significant decrease in PIF ($p<0.05$ for each group when compared to control) in all DFP-exposed animals during the 20-min exposure period. PEF decreased during exposure for all DFP-exposed animals, with significant ($p<0.05$ for each when compared to control) decreases in animals exposed to 9750, 12 200, and 14 625 mg × min/m^3 as compared to controls. During exposure, IT significantly ($p<0.05$ for each when compared to control) increased in animals exposed to 9750, 10 950, and 12 200 mg × min/m^3 while ET significantly ($p<0.05$ when compared to control) increased in animals exposed to 9750 mg × min/m^3 24 h post-exposure. TV decreased in all DFP-exposed animals during the exposure period with significant ($p<0.05$ when compared to control) decreases in animals exposed to 12 200 mg × min/m^3. As shown graphically in Figure 7, animals exposed to 9750, 10 950, 12 200, and 14 625 mg × min/m^3 DFP had significant ($p<0.05$ for each when compared to control) decreases in MV during the exposure period. No significant changes in any of these parameters were observed in control animals throughout the 24 h study period.

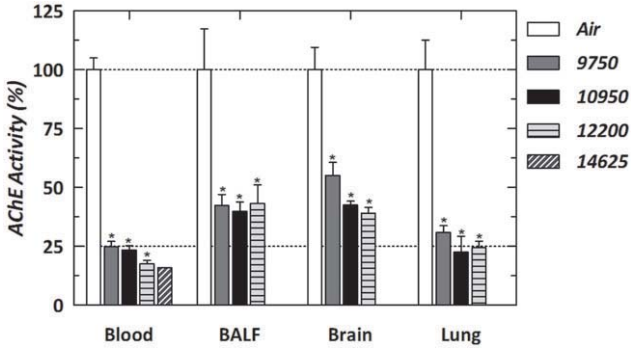

Figure 6. AChE activity at 24 h post-exposure to vapor DFP. $N=3$–6 for all groups except 14 625, for which $N=1$. (*$p<0.05$ for each when compared to control).

Discussion

Rationale

This exposure model was designed to be a more realistic representation of an actual exposure scenario in terms of exposure route and modeling of an at-risk population and to also generate data capable of bridging the gap between models based on different routes of exposure. The first step in determining the equivalence of data obtained from models utilizing different routes of exposure is a unit analysis of the obtained values.

In an actual exposure scenario, affected casualties would come into contact with varying concentrations of agent for varying periods of time. Mathematically, this is represented by a concentration-time product and described as an ''exposure dose'' in this model. Given in units of mg × min/m^3, the exposure dose is the total amount of agent to which the casualty is exposed but is not the toxicokinetically relevant dose, since individual differences in respiration and physiology will determine the amount of agent that is inhaled and

Table 2. Body weight-normalized respiratory parameters (as % of pre-exposure values).

		DFP exposure dose [mg × min/m^3]					
Parameter	Time point	0 (Air)	9750	10 950	12 200	14 625	19 500
Peak inspiratory flow (PIF)	Pre-exposure	100 ± 9	100 ± 12	100 ± 7	100 ± 16	100 ± 12	100 ± 8
	Exposure	93 ± 9	38 ± 7*	49 ± 7*	34 ± 4*	28 ± 5*	54 ± 10*
	24 h Post	108 ± 7	82 ± 17	118 ± N.D.	68 ± 22	N.D. ± N.D.	N.D. ± N.D.
Peak expiratory flow (PEF)	Pre-exposure	100 ± 6	100 ± 10	100 ± 10	100 ± 13	100 ± 8	100 ± 5
	Exposure	90 ± 6	50 ± 9*	68 ± 11	50 ± 7*	43 ± 6*	70 ± 11
	24 h Post	99 ± 6	56 ± 11	72 ± N.D.	41 ± 16*	N.D. ± N.D.	N.D. ± N.D.
Inspiratory time (IT)	Pre-exposure	100 ± 7	100 ± 6	100 ± 20	100 ± 9	100 ± 18	100 ± 8
	Exposure	101 ± 11	158 ± 14*	169 ± 30*	121 ± 11*	119 ± 11	97 ± 13
	24 h Post	82 ± 8	135 ± 39	92 ± N.D.	114 ± 3	N.D. ± N.D.	N.D. ± N.D.
Expiratory time (ET)	Pre-exposure	100 ± 4	100 ± 12	100 ± 16	100 ± 13	100 ± 11	100 ± 9
	Exposure	100 ± 4	110 ± 24	122 ± 15	93 ± 18	88 ± 12	84 ± 15
	24 h Post	125 ± 12	239 ± 57*	154 ± N.D.	175 ± 35	N.D. ± N.D.	N.D. ± N.D.
Tidal volume (TV)	Pre-exposure	100 ± 3	100 ± 5	100 ± 10	100 ± 11	100 ± 5	100 ± 10
	Exposure	91 ± 2	70 ± 12	91 ± 14	59 ± 7	51 ± 7*	70 ± 13
	24 h Post	89 ± 3	90 ± 4	85 ± N.D.	70 ± 2	N.D. ± N.D.	N.D. ± N.D.
Minute volume (MV)	Pre-exposure	100 ± 6	100 ± 10	100 ± 10	100 ± 9	100 ± 6	100 ± 6
	Exposure	92 ± 6	52 ± 6*	58 ± 6*	54 ± 2*	47 ± 7*	71 ± 9
	24 h Post	102 ± 6	66 ± 10	83 ± N.D.	64 ± 9	N.D. ± N.D.	N.D. ± N.D.

Pre-exposure ($N=6$), exposure ($N=6$) and 24 h post-exposure ($N=3$–6, except for 10 950 for which $N=1$). N.D. = not determined. (*$p<0.05$ when compared to 0 (Air) dose).

Table 3. Calculated exposure equivalent (CEE) [mg/kg].

	Exposure dose [mg × min/m^3]				
Method	9750	10 950	12 200	14 625	19 500
$\overline{CEE}$ (Average)	6.77 ± 0.82	8.06 ± 0.89	7.08 ± 0.29	9.17 ± 1.27	13.59 ± 1.67
$\int CEE$ (Exact)	6.81 ± 0.16	8.26 ± 0.33	7.28 ± 0.32	8.99 ± 0.36	13.80 ± 0.65

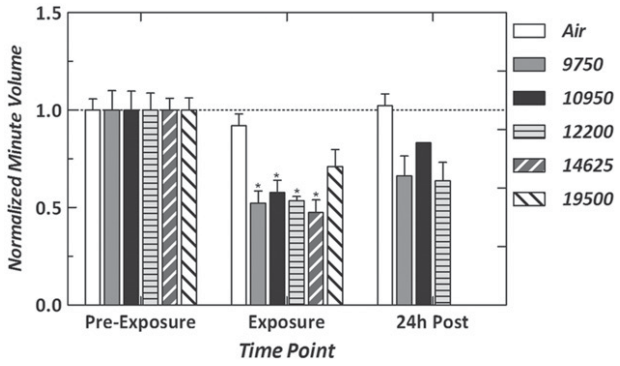

Figure 7. Minute volume (MV) for all animals. $N = 3$–6 for all groups except 14 625, for which $N = 1$. (*$p < 0.05$ for each when compared to control).

consequently absorbed into the body. Routes of exposure other than inhalation may offer a greater degree of control over the toxicokinetically relevant dose, but at the expense of increased realism in the model for an exposure scenario. However, this model works toward bridging the gap between these experiments by using the CEE as a method of translating an exposure dose from concentration-time units to a mass ratio.

Based on the previous mathematical basis for calculating CEE, Table 3 compares values for the CEE calculated using the exact form ($\int CEE$) with those obtained using averages ($\overline{CEE}$). Despite observing time-dependent behavior in both agent concentration in the chamber and MV, experimental data indicate that the utilization of averages is sufficient for determining the CEE. As the effective translation of the C_t into units of an administered dose, the CEE permits comparison of agent doses as administered using different routes of exposure and allows examination of how exposure doses relate to toxicokinetically relevant doses.

General observations

This study presents the development of a new vapor inhalation exposure model using the organophosphate DFP, which induces classical signs of organophosphate-induced toxicity, including neurotoxicity and alteration in respiratory dynamics. The induction of organophosphate-induced toxicity by this model suggests that it will be suitable for evaluating inhalational exposure to highly toxic CWNAs. In general, exposure to DFP resulted in increases in mortality corresponding to increases in dose. The LCt50 curve was determined by probit analysis to be 12 014 mg × min/m^3. Control animals all survived and showed no overt signs of toxicity. DFP-exposed animals exhibited a dose-dependent increase in body weight loss, an indication of acute toxicity, as well as increases in severity of the recorded clinical observations with increases in DFP dose. The cholinergic signs of DFP intoxication began to manifest approximately 7 to 10 min after the start of DFP exposure with chewing, licking and muscular fasciculations. Intoxication progressed to increased SLUD, and animals exposed to 10 950, 12 200, 14 625, and 19 500 mg × min/m^3 DFP developed significant to prominent muscular fasciculations and convulsions as well. Subcutaneous injections of DFP have been shown to also produce the typical signs of cholinergic intoxication, albeit with more prominent peripheral effects and less noticeable central nervous system effects (Gupta et al., 1985; Terry et al., 2011). The cholinergic signs of DFP intoxication in this study were similar to those described for CWNA exposure, but considerably different in terms of the severity and onset of intoxication. Differences in the nonspecific effects, affinity to central and peripheral AChE, variations in transport rate and degradation and metabolism of adequate concentrations to produce central nerve effects are the suggested reasons for the observed differences between DFP-induced and soman-induced intoxication (Gupta et al., 1985). Although previous studies have observed that organophosphates such as paraoxon and DFP inhibit AChE at a slower rate in comparison to CWNAs (Gupta et al., 1985; Wecker et al., 1978), the use of a less-toxic organophosphate has been a useful tool for the development of this inhalation model. This study will be used as a guideline for the establishment of a vapor-generating inhalation exposure model to evaluate CWNA-induced toxicity.

Animals exposed to DFP showed signs of acute toxicity and lung injury 24 h post-exposure in comparison to controls. Inhalation exposure to DFP resulted in inhibition of AChE activity in the blood, BALF, whole brain and lung tissues, and in general, at any given DFP dose, the inhibition of AChE at 24 h post-exposure was greatest in the blood, followed by the lung, the BALF and then the brain. Cardiac blood AChE activity was dose–dependently inhibited in DFP-exposed animals, and AChE activity at 24 h post-exposure ranged from 15% to 25%, as normalized to controls. Inhibition of BALF AChE activity was observed in all DFP animals, with activity at 24 h ranging from 40.0 ± 3.9 to 43.2 ± 8.0%. The AChE activity in lung and whole brain homogenates also exhibited dose-dependent inhibition in all DFP-exposed animals. The reduced AChE activities recorded in the cardiac blood at 24 h suggest that DFP vapor penetrates the blood stream via the respiratory tree. Likewise, the inhibition of whole brain AChE activity may be attributed to absorption of DFP through the bloodstream or delivery from the nose directly to the brain through the olfactory neuroepithelium. Further studies evaluating multiple agent doses and histological and biochemical analyses of various regions of the brain would be required to fully determine the effects of DFP on the brain. The observation of severe convulsions in

animals exposed to 14 625 and 19 500 mg × min/m^3 of DFP suggests that this model will be sufficient to serve as an additional exposure model for the evaluation of organophosphate- and CWNA-induced neurotoxicity. This is especially important in light of the fact that the majority of the models designed to evaluate CWNA neurotoxicity are based on subcutaneous injections (Atchison et al., 2004; Shih et al., 1994, 2005), and that any alteration in the route of exposure will produce differences in the timeframe governing the onset of toxicity. In turn, this implies the potential for required alterations in treatment strategies, which may also be explored using this exposure model.

Previous work established that nerve agent intoxication affects the respiratory system, regardless of the route of administration (Franz & Hilaski, 1990). However, the precise nature of the toxic effects of organophosphates and CWNAs on respiratory physiology and function following inhalation exposure is not well understood. In particular, the separate contributions of the peripheral nervous system and the central nervous center in CWNA-induced respiratory failure have not been well documented. For DFP, higher doses produced more significant alterations in the recorded respiratory parameters, and similarly, subcutaneous paraoxon exposure has been reported to also result in significant respiratory disturbance at higher doses (Villa et al., 2007).

All respiratory parameters were first normalized to their pre-exposure values and then to body weight, as the effect of body weight on respiratory parameters is well-documented (Alexander et al., 2008; Bide et al., 2000; Guyton, 1947) and is partially addressed through the use of weight-matched rats. Inhalation exposure to DFP simultaneously produced decreases in some respiratory parameters and increases in others as compared to control animals. On average, during exposure to DFP at all doses, PIF was reduced by approximately 60% and PEF by 40%, and TV decreased by an average of 30% and MV by 40%. Both IT and ET increased during exposure. A previous study (Vijayaraghavan et al., 1993) examining the effects of sensory irritants, airway constrictors and pulmonary irritants concluded that the type of agent could be characterized by patterns of changes in respiratory parameters. Based on those results, the changes in respiratory parameters caused by inhalation exposure to DFP are most similar to a mixture of those changes caused by airway constrictors and pulmonary irritants, and our observations of exposed animals do not contradict these findings. It is possible that increased airway secretions during and immediately after DFP exposure, in conjunction with other effects of inhibited AChE, contribute to increased lung resistance (not measured in this experiment) and airway obstruction. Of note is that at all exposure doses, the reduction in MV during exposure is still present at the 24 h endpoint (Figure 7).

Summary

This study describes the development of a new vapor inhalation exposure model for the exposure of conscious, untreated rats to chemical agents. The organophosphate DFP was used to establish the induction of classical cholinergic and respiratory toxicity following exposure to AChE-inhibiting compounds. The described exposure model is a flexible system and can be appropriately modified to deliver many different gases, volatile organics or mixtures thereof to more than two animals simultaneously. Based on the aims of the study, this model has the potential to accommodate the delivery of countermeasure strategies before, during or after exposure. Several of these modifications to the platform will be used to establish and evaluate cholinergic, respiratory and neurological toxicity in animals exposed to lethal concentrations of more potent CWNAs such as soman (GD). An improved understanding of these toxicological responses following vapor inhalational exposure to CWNA will then be utilized to evaluate and develop therapeutic countermeasures to protect military and civilian populations.

Declaration of interest

The work was supported by the Defense Threat Reduction Agency [3.F0014_09_RC_C]. This research was performed while the author (BW) held a National Research Council Research Associateship Award at USAMRICD. The views expressed in this article are those of the author(s) and do not reflect the official policy of the Department of Army, Department of Defense, or the U.S. Government.

References

Abbas F. (1984). Report of the specialists appointed by the Secretary-General of the United Nations to investigate allegations by the Islamic Republic of Iran concerning the use of chemical weapons. Arch Belg Suppl:302–10.

Alexander DJ, Collins CJ, Coombs DW, et al. (2008). Association of Inhalation Toxicologists (AIT) working party recommendation for standard delivered dose calculation and expression in non-clinical aerosol inhalation toxicology studies with pharmaceuticals. Inhal Toxicol 20:1179–89.

Anthony JS, Haley M, Manthei J, et al. (2004). Inhalation toxicity of Cyclosarin (GF) vapor in rats as a function of exposure concentration and duration: potency comparison to sarin (GB). Inhal Toxicol 16: 103–11.

Anzueto A, Berdine GG, Moore GT, et al. (1986). Pathophysiology of soman intoxication in primates. Toxicol Appl Pharmacol 86:56–68.

Atchison CR, Sheridan RE, Duniho SM, Shih TM. (2004). Development of a Guinea pig model for low-dose, long-term exposure to organophosphorus nerve agents. Toxicol Mech Meth 14:183–94.

Bajgar J. (2004). Organophosphates/nerve agent poisoning: mechanism of action, diagnosis, prophylaxis, and treatment. Adv Clin Chem 38: 151–216.

Benton BJ, McGuire JM, Sommerville DR, et al. (2006). Effects of whole-body VX vapor exposure on lethality in rats. Inhal Toxicol 18: 1091–9.

Bide RW, Armour SJ, Yee E. (2000). Allometric respiration/body mass data for animals to be used for estimates of inhalation toxicity to young adult humans. J Appl Toxicol 20:273–90.

Broughton E. (2005). The Bhopal disaster and its aftermath: a review. Environmental Health: A Global Access Science Source 4:6.

Dabisch PA, Davis EA, Renner JA, et al. (2008). Biomarkers of low-level exposure to soman vapor: comparison of fluoride regeneration to acetylcholinesterase inhibition. Inhal Toxicol 20:149–56.

Dunn MA, Sidell FR. (1989). Progress in medical defense against nerve agents. J Am Med Assoc 262:649–52.

Eckerman I. (2005). The Bhopal gas leak: analyses of causes and consequences by three different models. J Loss Prevent Process Indust 18:213–17.

Ellman GL, Courtney KD, Andres Jr V, Feather-Stone RM. (1961). A new and rapid colorimetric determination of acetylcholinesterase activity. Biochem Pharmacol 7:88–95.

Fawcett WP, Aracava Y, Adler M, et al. (2009). Acute toxicity of organophosphorus compounds in guinea pigs is sex- and age-

dependent and cannot be solely accounted for by acetylcholinesterase inhibition. J Pharmacol Exp Therapeut 328:516–24.
Feakes D. (2003). Global civil society and chemical and biological warfare. In Kaldor M, Anheier H, Glasius M, eds. Global civil society yearbook 2003. London, UK: LSE Global Governance.
Flegal KM, Carroll MD, Ogden CL, Curtin LR. (2010). Prevalence and trends in obesity among us adults, 1999–2008. J Am Med Assoc 303: 235–41.
Franz DR, Hilaski R. (1990). Sequence of cardiorespiratory effects of soman altered by route of administration. Toxicology Lett 51:221–5.
Gupta RC, Patterson GT, Dettbarn WD. (1985). Mechanisms involved in the development of tolerance to DFP toxicity. Fund Appl Toxicol 5: S17–28.
Guyton AC. (1947). Measurement of the respiratory volumes of laboratory animals. Am J Physiol 150:70–7.
Haigh JR, Lefkowitz LJ, Capacio BR, et al. (2008). Advantages of the WRAIR whole blood cholinesterase assay: comparative analysis to the micro-Ellman, Test-mate ChE, and Michel (DeltapH) assays. Chem Biol Interact 175:417–20.
Kirby RD, ed. (2005). Potential military chemical/biological agents and compounds. Washington, D.C.: Dept. of the Army.
Maynard RL, Chilcott RP. (2009). Toxicology of chemical warfare agents. In Ballantyne B, Marrs TC, Syversen T, eds. General and applied toxicology. 3rd ed. Hoboken (NJ): John Wiley and Sons Limited.
Mioduszewski R, Manthei J, Way R, et al. (2002a). Interaction of exposure concentration and duration in determining acute toxic effects of sarin vapor in rats. Toxicol Sci 66:176–84.
Mioduszewski RJ, Manthei JH, Way RA, et al. (2002b). Low-level sarin vapor exposure in rats: effect of exposure concentration and duration on pupil size [online]. Ft. Belvoir: Defense Technical Information Center. Available from: http://handle.dtic.mil/100.2/ADA402869 [last accessed 13 May 2013].
Muse WT, Thomson S, Crouse C, Matson K. (2006). Generation, sampling, and analysis for low-level GB (Sarin) and GF (Cyclosarin) vapor for inhalation toxicology studies. Inhal Toxicol 18:1101–8.
Niven AS, Roop SA. (2004). Inhalational exposure to nerve agents. Respir Care Clin N Am 10:59–74.
Phalen RF. (1976). Inhalation exposure of animals. Environ Health Perspect 16:17–24.
Redemann CE, Chaikin SW, Fearing RB, et al. (1948). The vapor pressures of forty-one fluorine-containing organic compounds. J Am Chem Soc 70:3604–6.
Rickett DL, Glenn JF, Beers ET. (1986). Central respiratory effects versus neuromuscular actions of nerve agents. Neurotoxicol 7:225–36.
Shih ML, McMonagle JD, Dolzine TW, Gresham VC. (1994). Metabolite pharmacokinetics of soman, sarin and GF in rats and biological monitoring of exposure to toxic organophosphorus agents. J Appl Toxicol 14:195–9.
Shih TM, Kan RK, McDonough JH. (2005). In vivo cholinesterase inhibitory specificity of organophosphorus nerve agents. Chem Biol Interact 157–8:293–303.
Sidell FR, Borak J. (1992). Chemical warfare agents: II. Nerve agents. Ann Em Med 21:865–71.
Sidell FR, Takafuji ET, Franz DR. (1997). Medical aspects of chemical and biological warfare. Washington (DC), Falls Church (VA), Fort Sam Houston (TX), Fort Detrick, Frederick (MD), Bethesda (MD): Borden Institute, Office of the Surgeon General, United States Army Medical Department Center and School; United States Army Medical Research and Material Command; Uniformed Services University of the Health Sciences.
Smithson AE, Levy L-A, Henry L. Stimson Center. (2000). Ataxia: the chemical and biological terrorism threat and the US response. Washington, DC: Henry L. Stimson Center.
Terry Jr AV, Buccafusco JJ, Gearhart DA, et al. (2011). Repeated, intermittent exposures to diisopropylfluorophosphate in rats: protracted effects on cholinergic markers, nerve growth factor-related proteins, and cognitive function. Neuroscience 176:237–53.
U.S. Census Bureau. (2010). Age and sex composition: 2010 census briefs. Washington, D.C.: U.S. Government Printing Office.
Vijayaraghavan R, Schaper M, Thompson R, et al. (1993). Characteristic modifications of the breathing pattern of mice to evaluate the effects of airborne chemicals on the respiratory tract. Arch Toxicol 67: 478–90.
Villa AF, Houze P, Monier C, et al. (2007). Toxic doses of paraoxon alter the respiratory pattern without causing respiratory failure in rats. Toxicology 232:37–49.
Wecker L, Kiauta T, Dettbarn WD. (1978). Relationship between acetylcholinesterase inhibition and the development of a myopathy. J Pharmacol Exp Ther 206:97–104.

Appendices

Appendix A. Agent concentration in the exposure chamber

Variables

m = Mass of agent in chamber at any time
t = Time
V_t = Volume of exposure chamber
C_i = Agent concentration entering chamber
C_t = Agent concentration inside chamber
F_i = Flow rate into chamber
F_o = Flow rate out of chamber
C = Concentration of agent

Mass balance for filling the exposure chamber during time interval dt:

Change in mass = mass in − mass out
Change in mass = (volume in)(concentration in) − (volume out)(concentration out)
Change in mass = (flow rate in)(time interval)(C_i) − (flow rate out)(time interval)(C_t)
(Change in mass)/(time interval) = (F_i)(C_i) − (F_o)(C_t)

In the limit as the time interval approaches zero:

$$\frac{dm}{dt} = F_iC_i - F_oC_t \tag{1}$$

Given $m = C_tV_t$ and using the product rule:

$$\frac{d(C_tV_t)}{dt} = C_t\frac{dV_t}{dt} + V_t\frac{dC_t}{dt} = F_iC_i - F_oC_t \tag{2}$$

$$V_t\frac{dC_t}{dt} = F_iC_i - F_oC_t = F_o\left(\frac{F_iC_i}{F_o} - C_t\right) \tag{3}$$

$$\frac{dC_t}{dt} = \frac{F_o}{V_t}\left(\frac{F_iC_i}{F_o} - C_t\right) \tag{4}$$

Separating and integrating C_t from 0 to C:

$$\int_0^C \frac{dC_t}{\left(\frac{F_iC_i}{F_o} - C_t\right)} = \frac{F_o}{V_t}\int_0^t dt \tag{5}$$

$$-\ln\left(\frac{F_iC_i}{F_o} - C\right) + \ln\left(\frac{F_iC_i}{F_o}\right) = \frac{F_o}{V_t}(t-0) \tag{6}$$

$$\ln\left(\frac{F_iC_i}{F_o} - C\right) = \ln\left(\frac{F_iC_i}{F_o}\right) - \frac{F_o}{V_t}t \tag{7}$$

$$e^{\ln\left(\frac{F_iC_i}{F_o} - C\right)} = e^{\ln\left(\frac{F_iC_i}{F_o}\right)}e^{-\frac{F_o}{V_t}t} \tag{8}$$

$$\left(\frac{F_iC_i}{F_o} - C\right) = \frac{F_iC_i}{F_o}e^{-\frac{F_o}{V_t}t} \tag{9}$$

$$C = \frac{F_iC_i}{F_o} - \frac{F_iC_i}{F_o}e^{-\frac{F_o}{V_t}t} \tag{10}$$

Defining the steady-state concentration, C_{SS}, and rate constant, k:

$$C_{SS} = \frac{F_iC_i}{F_o} \tag{11}$$

$$k = \frac{F_o}{V_t} \tag{12}$$

The agent concentration in the exposure chamber during agent filling, as a function of time, is:

$$C = C_{SS}\left(1 - e^{-kt}\right) \tag{13}$$

For the emptying of the chamber, the mass balance is identical to the filling, except that $F_i = 0$ during this phase. Mass balance is:

$$\frac{dm}{dt} = F_i C_i - F_o C_t \tag{14}$$

Again using $m = C_t V_t$ and the product rule, substituting $F_i = 0$:

$$\frac{d(C_t V_t)}{dt} = C_t \frac{dV_t}{dt} + V_t \frac{dC_t}{dt} = F_i C_i - F_o C_t \tag{15}$$

$$V_t \frac{dC_t}{dt} = -F_o C_t \tag{16}$$

$$\frac{dC_t}{dt} = -\frac{F_o}{V_t} C_t \tag{17}$$

Separating and integrating, with C_1 equal to C_t evaluated at time t_1, which corresponds to the length of the exposure:

$$\int_{C_1}^{C} \frac{dC_t}{C_t} = -\frac{F_o}{V_t} \int_{t_1}^{t} dt \tag{18}$$

$$\ln C - \ln C_1 = \ln \frac{C}{C_1} = -\frac{F_o}{V_t}(t - t_1) \tag{19}$$

$$e^{\ln \frac{C}{C_1}} = e^{-\frac{F_o}{V_t}(t - t_1)} \tag{20}$$

$$C = C_1 e^{-\frac{F_o}{V_t}(t - t_1)} \tag{21}$$

With $k = -F_o/V_t$, and $C_1 = C_{SS}\left(1 - e^{-kt}\right)|_{t_1}$, the agent concentration in the exposure chamber during agent venting, as a function of time, is:

$$C = C_1 e^{-k(t - t_1)} \tag{22}$$

Appendix B. Theoretical agent use during exposure

Constants

P_{atm} = [mmHg] Atmospheric pressure at experimental altitude
MW_{DFP} = [g mol^{-1}] Molecular weight, DFP
ρ_{DFP} = [g cm^3] Density, DFP
R = [L mmHg $K^{-1} mol^{-1}$] Ideal gas constant
T_{ref} = [K] Standard reference temperature
P_{ref} = [psia] Standard reference pressure
P_{N2reg} = [psig] Nitrogen tank pressure

Antoine Equation Parameters for DFP (Redemann et al., 1948*)*

A = 8.872
B = 2671
C = 273.15

Calculating vapor pressure of DFP @ T = 22.5 °C using the Antoine Equation:

$$P_{mmHg} = 10^{A - \frac{B}{C+T}} \tag{1}$$

With $P_{DFP} = 0.688$ mmHg, the saturated vapor stream exiting the saturator cell (equivalent, concentration of DFP in the stream to the exposure chamber), C_i, will contain:

$$[DFP]_{\max} = \frac{VP_{DFP}}{P_{atm}} = 905 \text{ ppm} \tag{2}$$

$$[DFP]_{\max} = \frac{[DFP_{[ppm]}] P_{atm} MW_{DFP}}{RT} \tag{3}$$

$$[DFP]_{\max} = 6873 \text{ mg m}^{-3} \tag{4}$$

For a given flow rate out of the saturator cell (equivalently, flow rate into the exposure chamber), F_i can be converted from SLPM to LPM at experimental conditions:

$$F_{i[LPM]} = \frac{T}{T_{ref}} \times \frac{P_{ref}}{P_{N2reg}} \times F_{i[SLPM]} \tag{5}$$

$$F_{i[LPM]} = 1.070 \text{ L min}^{-1} \tag{6}$$

The total mass or volume of agent used in an exposure can therefore be calculated for a given experimental time, $t = 20$ min, yielding:

$$m_{DFP} = F_i \times C_i \times t = 147 \text{ mg} \tag{7}$$

$$V_{DFP} = \frac{m_{DFP}}{\rho_{DFP}} = 0.139 \text{ mL} \tag{8}$$

Appendix C. Exposure Chamber Behavior

Within the chamber, the time required to reach 95% or 99% of the steady state concentration of DPF, C_{SS}, can be determined at experimental conditions. Using Equations (11), (12), and (13) from Appendix A:

$$C = C_{SS}\left(1 - e^{-kt}\right) \tag{1}$$

$$1 - \frac{C}{C_{SS}} = e^{-kt} \tag{2}$$

$$t = -\frac{1}{k} \ln\left(1 - \frac{C}{C_{SS}}\right) \tag{3}$$

Thus, the required time is a function of the chamber exit flow, F_o. For our conditions:

$$t_{95\%} = 4.4 \text{ min} \tag{4}$$

$$t_{99\%} = 6.7 \text{ min} \tag{5}$$